European Radiology (2019) 29:4783–4793
https://doi.org/10.1007/s00330-019-06032-y

IMAGING INFORMATICS AND ARTIFICIAL INTELLIGENCE

Modified calcium subtraction in dual-energy CT angiography of the lower extremity runoff: impact on diagnostic accuracy for stenosis detection

Domenico De Santis[1,2] · Carlo N. De Cecco[1] · U. Joseph Schoepf[1] · John W. Nance[1] · Ricardo T. Yamada[1] · Brooke A. Thomas[1] · Katharina Otani[3] · Brian E. Jacobs[1] · D. Alan Turner[1] · Julian L. Wichmann[4] · Marwen Eid[1] · Akos Varga-Szemes[1] · Damiano Caruso[2] · Katharine L. Grant[5] · Bernhard Schmidt[6] · Thomas J. Vogl[4] · Andrea Laghi[2] · Moritz H. Albrecht[1,4]

Received: 7 August 2018 / Revised: 21 December 2018 / Accepted: 22 January 2019 / Published online: 25 February 2019

Abstract

Objectives To investigate the diagnostic accuracy of a modified three-material decomposition calcium subtraction (CS) algorithm for the detection of arterial stenosis in dual-energy CT angiography (DE-CTA) of the lower extremity runoff compared to standard image reconstruction, using digital subtraction angiography (DSA) as the reference standard.

Methods Eighty-eight patients (53 males; mean age, 65.9 ± 11 years) with suspected peripheral arterial disease (PAD) who had undergone a DE-CTA examination of the lower extremity runoff between May 2014 and May 2015 were included in this IRB-approved, HIPAA-compliant retrospective study. Standard linearly blended and CS images were reconstructed and vascular contrast-to-noise ratios (CNR) were calculated. Two independent observers assessed subjective image quality using a 5-point Likert scale. Diagnostic accuracy for ≥ 50% stenosis detection was analyzed in a subgroup of 45 patients who had undergone additional DSA. Diagnostic accuracy parameters were estimated with a random-effects logistic regression analysis and compared using generalized estimating equations.

Results CS datasets showed higher CNR (15.3 ± 7.3) compared to standard reconstructions (13.5 ± 6.5, $p < 0.001$). Both reconstructions showed comparable qualitative image quality scores (CS, 4.64; standard, 4.57; $p = 0.220$). Diagnostic accuracy (sensitivity, specificity, positive and negative predictive values) for CS reconstructions was 96.5% (97.5%, 95.6%, 90.9%, 98.1) and 93.1% (98.8%, 90.4%, 82.3%, 99.1%) for standard images.

Conclusions A modified three-material decomposition CS algorithm provides increased vascular CNR, equivalent qualitative image quality, and greater diagnostic accuracy for the detection of significant arterial stenosis of the lower extremity runoff on DE-CTA compared with standard image reconstruction.

Key Points

- *Calcified plaques may lead to overestimation of stenosis severity and false positive results, requiring additional invasive digital subtraction angiography (DSA).*
- *A modified three-material decomposition algorithm for calcium subtraction provides greater diagnostic accuracy for the detection of significant arterial stenosis of the lower extremity runoff compared with standard image reconstruction.*
- *The application of this algorithm in patients with heavily calcified vessels may be helpful to potentially reduce inconclusive CT angiography examinations and the need for subsequent invasive DSA.*

✉ U. Joseph Schoepf
schoepf@musc.edu

[1] Department of Radiology and Radiological Science, Medical University of South Carolina, 25 Courtenay Drive, Charleston, SC, USA

[2] Department of Radiological Sciences, Oncology and Pathology, Sant'Andrea University Hospital, "Sapienza" - University of Rome, Rome, Italy

[3] Imaging and Therapy Systems Division, Healthcare Sector, Siemens Japan K.K., Tokyo, Japan

[4] Division of Experimental and Translational Imaging, Department of Diagnostic and Interventional Radiology, University Hospital Frankfurt, Frankfurt am Main, Germany

[5] Siemens Medical Solutions USA, Inc, Malvern, PA, USA

[6] Division of Computed Tomography, Siemens Healthineers, Forchheim, Germany

Keywords Computed tomography angiography · Peripheral arterial disease · Lower extremity · Constriction, pathologic · Sensitivity and specificity

Abbreviations

CM	Contrast media
CNR	Contrast-to-noise ratio
CS	Calcium subtraction
CTA	CT angiography
DE-CTA	Dual-energy CT angiography
DSA	Digital subtraction angiography
ICCs	Intraclass correlation coefficients
NPV	Negative predictive value
PAD	Peripheral arterial disease
PPV	Positive predictive value

Introduction

CT angiography (CTA) of the lower extremity runoff is widely used as a robust and non-invasive imaging modality for the evaluation of peripheral arterial disease (PAD) [1]. However, extensive calcifications of the arterial vasculature remain a diagnostic challenge in CTA, as calcified plaques frequently cause blooming artifacts and partial volume effects that can result in an overestimation of stenosis severity and false positive results [2, 3]. In cases of diagnostic uncertainty, additional invasive digital subtraction angiography (DSA) is commonly performed as the reference standard for the assessment of arterial stenosis [4]. However, DSA may incur patient discomfort [5], potential complications in up to 7% of cases [6], higher costs [7], and increased radiation exposure [6, 8].

Dual-energy CT simultaneously acquires imaging data using both high and low tube voltages [9, 10]. Since materials are defined by their specific attenuation characteristics at different tube potentials [11], this approach enables material decomposition and the differentiation of calcium from intravascular iodine based on a single CTA acquisition [12–14]. Thus, a modified three-material decomposition algorithm for calcium subtraction (CS) has been recently developed, allowing for the accurate removal of calcified extracranial carotid artery plaques [15] and improved luminal visualization of coronary arteries [16]. Accordingly, we hypothesized that this technique may have incremental value for the assessment of arterial stenosis of the lower extremities.

Therefore, the aim of our study was to investigate the diagnostic accuracy of the modified CS algorithm for arterial stenosis detection in dual-energy CT angiography (DE-CTA) of the lower extremity runoff compared to standard image reconstruction, using digital subtraction angiography (DSA) as the reference standard.

Materials and methods

Patient population

This retrospective, single-center study was approved by our local institutional review board with a waiver of informed consent and conducted in compliance with the HIPAA.

Institutional databases were reviewed to identify patients who underwent a clinically indicated DE-CTA examination of the lower extremity runoff for known or suspected PAD between May 2014 and May 2015. Exclusion criteria included motion artifacts hindering adequate image analysis, incomplete DE-CTA examinations, and any deviation from the contrast medium (CM) injection protocol. Patients with lower extremity amputations or stented vessels were not excluded from the study.

CTA image acquisition

All examinations were performed using a third-generation dual-source CT scanner (SOMATOM Force, Siemens Healthineers) operated in dual-energy mode. Image acquisition was performed in the craniocaudal direction with a scan length ranging from the infrarenal abdominal aorta to the toes. A 120-kVp bolus-tracking acquisition (CARE Bolus, Siemens) was used to determine scan initiation by placing a region-of-interest (ROI) in the abdominal descending aorta at the level of the renal arteries with a trigger threshold of 115 Hounsfield units (HU) and 7-s delay. Scanning parameters were as follows: pitch, 0.7; detector collimation, $2 \times 64 \times 0.6$ mm with z-flying focal spot technique; field of view, 350 mm. Tubes A and B were operated with 90 and 150 kVp, 95 and 59 reference mAs, respectively. Tin prefiltration and automated tube current modulation software (CARE Dose 4D, Siemens) were used.

For each examination, 0.9 mL/kg of CM (320 mg/mL iodixanol; Visipaque, GE Healthcare) with a maximum of 90 mL was intravenously administered through a 20-gauge cannula placed in a vein of the antecubital fossa. An automated dual-syringe power injector (Stellant D CT Injection System, Medrad, Inc.) was used with a flow rate of 3.0 mL/s.

DE-CTA image reconstruction

Transverse low- and high-kVp DE-CTA imaging data were reconstructed using a medium sharp convolution kernel (Qr40) and iterative reconstruction software (ADMIRE, Siemens; strength, 3) [17], 512^2-pixel matrix size, and 350 mm reconstruction field-of-view. Standard DE-CTA

images were reconstructed as linearly blended M_0.5 images by merging 50% of the low-kV and 50% of the high-kV data [18], both as multi-planar reformats (MPR; thickness, 1.5 mm; increment, 1.0 mm) and maximum-intensity projections (MIP; thickness, 10.0 mm; increment, 1.0 mm) in transverse, oblique coronal, and sagittal orientation.

DE-CTA datasets were uploaded to a prototype software environment (eXamine version 0.9.12.23196, Siemens) for CS reconstruction using the same parameters. The software is based on a modified dual-energy three-material decomposition algorithm as recently described [15, 16]. In brief, this algorithm considers calcium as a primary material, theoretically allowing for complete and selective calcium subtraction without affecting the extent of iodine-attenuated lumina. In contrast, traditional methods recognize iodine and soft tissue/water as basic substances of the initial spectral decomposition.

The standard and CS MPR and MIP reconstructions were transferred to a 3D multi-modality workstation (*syngo*.via version VB10B; Siemens) for further analysis.

Digital subtraction angiography

Invasive DSA was performed in a subgroup of patients (n = 45) within 30 days of DE-CTA. These examinations were performed by a radiologist with 6 years of experience in DSA (RTY) using a robotic angiography system (Axiom Artis, Siemens) via a trans-femoral approach. The catheter tip (5-F Omni Flush catheter; AngioDynamics) was positioned at the level of the distal abdominal aorta, and 90 mL of CM (320 mgI/mL iodixanol; Visipaque, GE Healthcare) was injected. Step-table acquisitions in a postero-anterior projection were performed to evaluate pelvic and lower extremity arteries, with additional 30° left and right anterior oblique projections at the level of the iliac and common femoral arteries.

Objective image quality analysis

Measurements were performed by an observer with 4 years of experience in CTA (ME) using transverse standard and CS MPR images. Intravascular attenuation values were recorded following an 18-segment model by placing ROIs in the following vessel segments: (1) supraceliac aorta, (2) distal aorta, (3 + 4) common iliac arteries, (5 + 6) common femoral arteries, (7 + 8) superficial femoral arteries, (9 + 10) popliteal arteries, (11 + 12) anterior tibial arteries, (13 + 14) tibioperoneal trunks, (15 + 16) posterior tibial arteries, and (17 + 18) peroneal arteries. Average values are based on all the aforementioned arterial segments. For further subgroup analysis, segments were grouped as follows: (1 + 2) *aortic*, (3 to 8) *iliofemoral*, and (9 to 18) *lower leg arteries* [19].

ROIs were drawn as large as possible, avoiding the vessel wall, plaques, and stent portions. In partially occluded vessel segments, the ROI was placed proximal to the occlusion. Segments with severe stenosis or total occlusion rendering ROI measurements impossible were excluded from the objective image quality analysis but still evaluated for subjective image quality and diagnostic accuracy. Vessels with suboptimal contrast attenuation were not excluded. Image noise was defined as the mean standard deviation (SD) of attenuation (HU) in a ROI (size, 2 cm^2) in the retroperitoneal fat. Furthermore, the attenuation of the psoas muscle at the L5 level was determined. All ROIs were measured three times and averaged to minimize measurement inaccuracies.

Contrast-to-noise ratio (CNR) was calculated as follows [19]:

$$CNR = \frac{HU_{\text{artery}} - HU_{\text{muscle}}}{SD_{\text{fat}}}$$

Subjective image quality analysis

Two observers with 5 (DDS) and 11 (CNDC) years of experience in CTA blinded to clinical information and previous reports independently performed a qualitative image analysis using all available reconstructions. Images were evaluated in a randomized order with freely adjustable window settings. In the main subjective analysis, observers were asked to grade visualization of the contrast-enhanced arterial lumen (Table 1). In addition, the CS reconstructions were dichotomously evaluated on a per-patient basis to assess the presence of: (1) calcium over-subtraction, (2) calcium under-subtraction, (3) effect on non-calcified plaques, and (4) difficulties in the interpretation of stented segments. To minimize recall bias, only a single randomly chosen image series (Standard or CS) from each patient was analyzed during each interpretation and a time interval of at least 14 days was maintained between sessions.

Diagnostic accuracy

A radiologist with 6 years of DSA experience (RTY), aware of patient clinical information but blinded to CTA results, interpreted DSA images using the aforementioned 18-segment model. For the purpose of this study, vessel segment lesions were categorized as non-significant (0–49% luminal narrowing) or significant (50–100% luminal narrowing) [19]. Arterial stenosis was graded with an electronic caliper. In cases with multiple arterial stenoses in a single segment, the stenosis with the highest grade was evaluated.

To assess the diagnostic accuracy of the standard DE-CTA and CS reconstructions, both datasets were evaluated after a 6-week interval by the two observers who had performed the

Table 1 5-point scale for subjective image quality based on arterial contrast attenuation

Score	Score determinants
1	Poor opacification, stenosis evaluation is not possible
2	Suboptimal opacification, stenosis evaluation is only possible in the major runoff arteries
3	Acceptable opacification, diagnostic for the complete runoff but with low confidence
4	Good opacification, diagnostic for the complete runoff with high confidence
5	Excellent opacification until the smallest runoff arteries, excellent diagnostic confidence

subjective image quality analysis. Observers were asked to independently evaluate each segment for the presence of insignificant or significant stenosis using the aforementioned approach. Disagreement regarding lesion significance was resolved during a consensus interpretation session 7 days later.

CTA radiation dose

The CT dose index volume ($CTDI_{vol}$) and dose-length-product (DLP) were recorded from the automatically provided scan protocol. Effective dose was calculated by multiplying the DLP by gender-specific k conversion coefficients (k_{male} = 0.0056, k_{female} = 0.0068) [20].

Statistical analysis

Statistical comparisons were performed using commercially available software (IBM Corp. Released 2016. IBM SPSS Statistics for Windows, Version 24.0. IBM Corp.; Stata14, StataCorp LP). For all numerical values derived from multiple measurements, the mean value and SD were calculated. The Kolmogorov-Smirnov test was used to assess the normality of data distribution. The Wilcoxon signed-rank test and the Student t test were used to analyze non-Gaussian and Gaussian data, respectively.

The subjective image quality scores averaged from the two observers were compared with the Mann-Whitney U test. The absolute agreement was calculated in a patient-based fashion by means of intraclass correlation coefficients (ICCs) using a two-way mixed model and was interpreted as follows: ICC ≤ 0.20, slight; ICC = 0.21–0.40, fair; ICC = 0.41–0.60, moderate, ICC = 0.61–0.80, substantial; and ICC = 0.81–1.0, excellent agreement [21].

Random-effects logistic regression was used to estimate sensitivity, specificity, overall diagnostic accuracy, positive predictive value (PPV), and negative predictive value (NPV) of each image reconstruction algorithm and were subsequently compared [22]. Diagnostic accuracy parameters were compared using generalized estimating equations. An exchangeable correlation working matrix was assumed to model the correlation between the segments. A robust variance estimator was included in the model to correct for misspecifications of the correlation matrix [22].

A two-tailed $p < 0.05$ was considered statistically significant.

Results

Patient population

Comprehensive results of patient characteristics are reported in Table 2. Of the 106 patients initially identified, 18 subjects were excluded due to motion artifact ($n = 1$),

Table 2 Patient characteristics

Clinical data	Value
No. of patients	88
Mean age (years)*	
All	65.9 ± 11.8 (19–94)
Male	67.5 ± 8.8 (45–85)
Female	63.6 + 15.0 (19–94)
Sex†	
Male	52 (59.1)
Female	36 (40.9)
BMI (kg/m^2)*	
All	27.5 ± 6.4 (16.6–45.2)
Male	27.4 ± 5.7 (16.6–43.8)
Female	27.7 ± 7.5 (16.6–45.2)
Cardiovascular risk factors†	
Hypertension	71 (80.7)
Dyslipidemia	70 (79.5)
Current or former smoking	77 (87.5)
Diabetes mellitus	31 (35.2)
Coronary artery disease	51 (58.0)
Fontaine classification†	
Stage I	26 (29.5)
Stage IIA	17 (19.3)
Stage IIB	29 (33.0)
Stage III	9 (10.2)
Stage IV	7 (8.0)

BMI, body mass index

*Data are mean ± standard deviation (range)

† Data are number of patients (%)

incomplete examinations ($n = 2$), deviations from the CM injection protocol ($n = 4$), or failure to retrieve the entire DE-CTA raw data ($n = 11$). Thus, a total of 88 patients (52 males) with a mean age of 65.9 ± 11.8 years (range 19–94 years) and body mass index of 27.5 ± 6.4 kg/m^2 were included (Fig. 1). Three patients had undergone prior unilateral leg amputation above ($n = 1$) or below the knee ($n = 2$). Twenty-seven subjects had undergone prior stent implantation.

A subgroup of 45 patients underwent invasive DSA within 9.4 ± 5.7 days (range, 0–25 days) of DE-CTA examination. During the time interval between DE-CTA and DSA, patients did not receive surgical or interventional treatment, begin new medications, or initiate other types of therapy.

Since three patients underwent unilateral leg amputation, 13 segments were unavailable for analysis, resulting in a total of 1571 evaluable segments. Among them, 92 (6%) occluded segments were excluded from the objective image quality assessment (due to ROI feasibility issues) but were included in the diagnostic accuracy analysis. Among these 1479 segments, 54 (4%) were stented and included in both the objective image quality assessment and diagnostic accuracy evaluation.

In the subgroup of 45 patients who underwent additional DSA, 533 arterial segments, of which 14 (3%) were stented, were available for assessment of diagnostic accuracy, resulting in an average of 12 segments per subject (range, 1–18 segments).

Table 3 Objective image quality scores of calcium-subtracted images and standard DE-CTA reconstructions. All differences were significant ($p \leq 0.001$)

	CS	Standard
Vessel attenuation*		
Average	223.0 ± 67.9	271.1 ± 65.4
Aortic	280.5 ± 82.0	311.2 ± 73.6
Iliofemoral	264.0 ± 83.8	297.6 ± 73.2
Lower leg arteries	182.4 ± 65.7	245.3 ± 67.4
Muscle attenuation*	− 40.4 ± 17.5	52.5 ± 8.7
Noise	19.5 ± 5.8	17.8 ± 4.4
CNR		
Average	15.3 ± 7.3	13.5 ± 6.5
Aortic	18.6 ± 8.7	15.8 ± 7.3
Iliofemoral	17.6 ± 8.6	15.1 ± 7.2
Lower leg arteries	13.1 ± 6.7	12.0 ± 6.2

Data are mean ± standard deviation. Average values derive from all 18 measured arterial segments; aortic values derive from segments 1 and 2; iliofemoral values are calculated in segments from 3 to 8, and lower leg values include segments from 9 to 18. All differences were significant ($p \leq 0.001$)

CNR, contrast-to-noise ratio; *CS,* calcium-subtracted images; *Standard,* linearly blended images

*Hounsfield units

Significant stenosis was observed in 163 segments (31%), whereas 370 segments (69%) were considered non-significant.

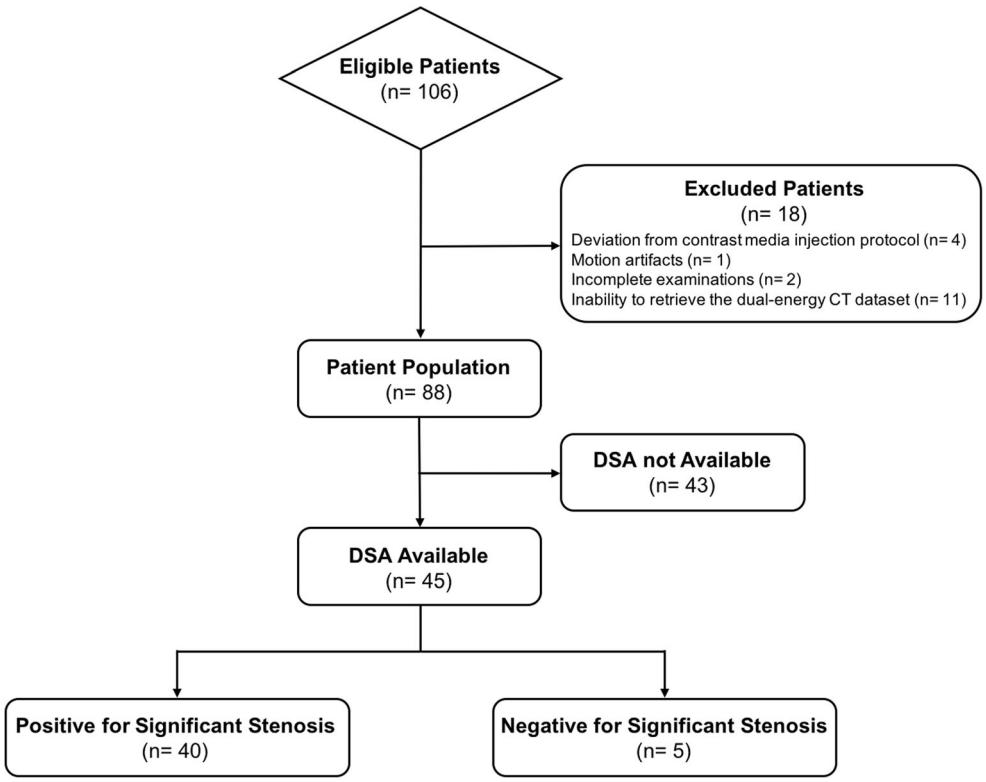

Fig. 1 Flow diagram of patient recruitment. DSA served as the reference standard. DSA, digital subtraction angiography

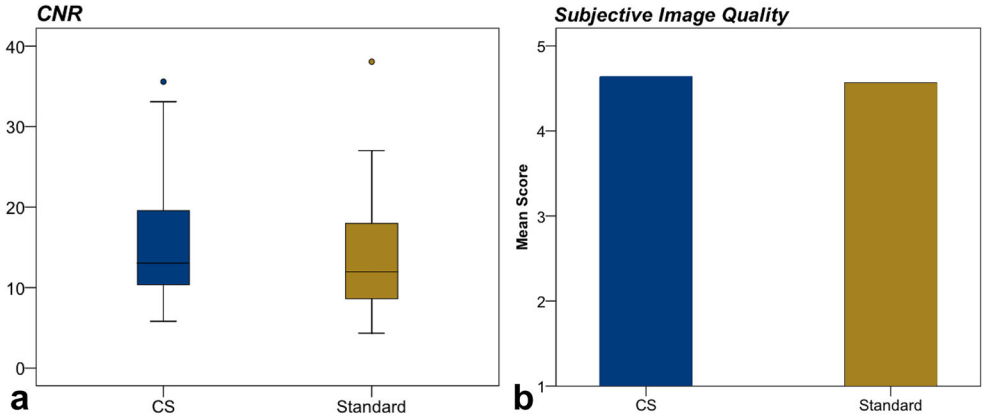

Fig. 2 Box-and-whisker plots for quantitative image quality parameters. The calcium-subtracted (CS) datasets provided a greater contrast-to-noise ratio (**a**) compared to the standard dual-energy CT angiography reconstructions ($p < 0.001$). Furthermore, observers' scores revealed equivalent image quality (**b**) between CS and standard reconstructions ($p = 0.220$). Boxes represent the middle 50% of the data and solid lines represent the median, whiskers represent minimum and maximum values, and dots represent the outliers. CNR, contrast-to-noise ratio; HU, Hounsfield units

No CM-related adverse reactions following DE-CTA or DSA occurred. One patient showed post-procedural bleeding in the groin following DSA.

Objective image quality analysis

Detailed results are summarized in Table 3 and Fig. 2a. The CS reconstructions showed lower vessel attenuation (223.0 ± 67.9 HU) compared to the standard DE-CTA images (271.0 ± 65.4 HU, $p < 0.001$). Likewise, the CS algorithm reconstructions showed significantly lower muscle attenuation (− 40.4 ± 17.5 HU) compared to the standard DE-CTA datasets (52.5 ± 8.7 HU, $p < 0.001$). The resultant CNR in CS images was significantly higher in comparison to the standard DE-CTA datasets (mean CNR, 15.3 ± 7.3 vs. 13.5 ± 6.5, $p < 0.001$).

Subjective image quality analysis

Comprehensive data are reported in Table 4 and Fig. 2b. Scores for subjective image quality of CS and standard DE-CTA datasets were comparable (4.30 ± 0.84 vs. 4.26 ± 0.94, $p = 0.895$). ICC for the assessment of both reconstructions was excellent (0.879 and 0.897). Observers found over-subtraction of calcium in 1 patient (1.1%) and under-subtraction of calcium in 3 subjects (3.4%) for the CS reconstructions. An impact of non-calcified plaques or substantial difficulties in the interpretation of stented segments was not observed.

Diagnostic accuracy

Detailed results are listed in Table 5 and shown in Fig. 3. The CS algorithm resulted in a significantly greater diagnostic accuracy for the detection of significant arterial stenosis compared to standard DE-CTA image series (96.5 vs. 93.1%, $p = 0.004$). Sensitivity (97.5 vs. 98.8%, $p = 0.570$) and NPV (98.1 vs. 99.1%, $p = 0.740$) were comparable among both reconstructions. CS image series allowed for significantly greater specificity and PPV compared to standard DE-CTA reconstructions (95.6 vs. 90.4%, $p = 0.001$, and 90.9 vs. 82.3%, $p = 0.010$, respectively) (Figs. 4 and 5).

Table 4 Subjective image quality and inter-observer agreement of calcium-subtracted images and standard DE-CTA reconstructions

	CS	Standard	*p* value
Score*	4.30 ± 0.84	4.26 ± 0.94	0.895
ICC†	0.879 (0.813–0.921)	0.897 (0.843–0.932)	

CS, calcium-subtracted images; *ICC,* intraclass correlation coefficient; *Standard,* linearly blended images

*Data are mean ± standard deviation

† Data are mean (95% confidence interval)

Table 5 Per-segment diagnostic accuracy results of calcium-subtracted images and standard DE-CTA reconstructions

	CS	Standard	*p* value
Accuracy	96.5 (94.4–98.5)	93.1 (90.2–96.0)	*0.004*
Sensitivity	97.5 (93.6–100)	98.8 (97.6–100)	0.570
Specificity	95.6 (92.6–98.6)	90.4 (86.0–94.8)	*0.001*
Positive predictive value	90.9 (86.9–96.3)	82.3 (75.9–89.5)	*0.010*
Negative predictive value	98.1 (94.6–100)	99.1 (97.3–100)	0.740

Data are mean (95% confidence interval); significant differences are in *italic*

CS, calcium-subtracted images; *Standard,* linearly blended images

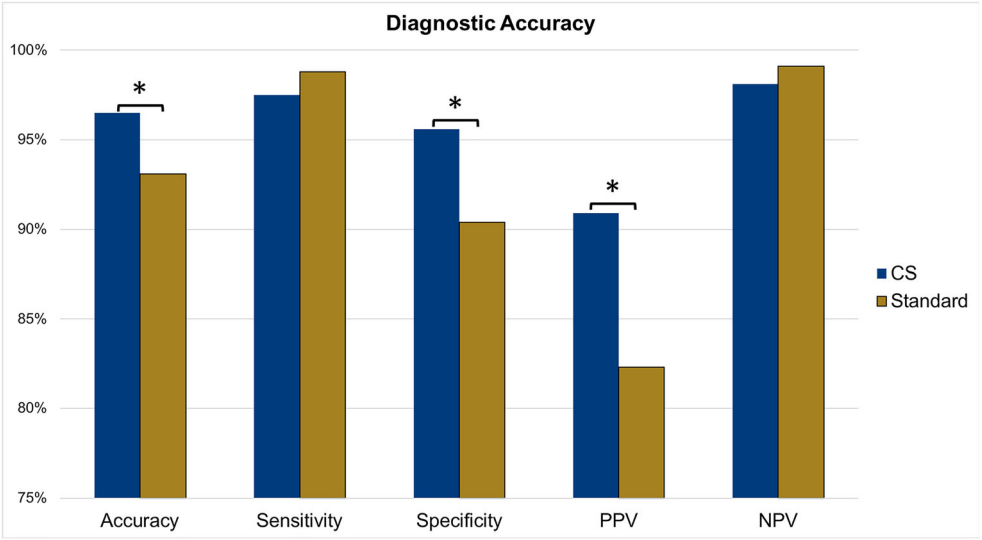

Fig. 3 Bar graphs depicting diagnostic accuracy for the detection of ≥ 50% arterial stenosis of calcium-subtracted (CS) and standard dual-energy CT angiography reconstructions. The CS algorithm showed higher overall diagnostic accuracy ($p = 0.004$), specificity ($p = 0.001$), and positive predictive value ($p = 0.010$) (asterisks). PPV, positive predictive value; NPV, negative predictive value

Radiation dose

Average $CTDI_{vol}$ of all examinations was 4.3 ± 1.7 mGy and mean DLP was 581.3 ± 234.7 mGy cm, resulting in an average effective dose of 3.5 ± 1.6 mSv.

Discussion

In current clinical practice, the extent and severity of PAD are commonly assessed by means of CTA, magnetic resonance angiography (MRA), and duplex sonography [23–25]. Duplex sonography is easily accessible and inexpensive compared to the other aforementioned techniques, but the accuracy may be limited in the presence of multi-level occlusive disease, severe arterial calcification, and the related acoustic shadowing [26]. Additionally, this technique may be operator-dependent and relatively time-consuming [24]. CTA and MRA are listed in the same class of recommendation by the latest European [27] and American guidelines [28], while the favorable indications for each technique have been reported comprehensively [29]. Nevertheless, MRA can be limited in the scenario of stents and by technical challenges such as the proper selection of the direction of flow-spoiling gradients,

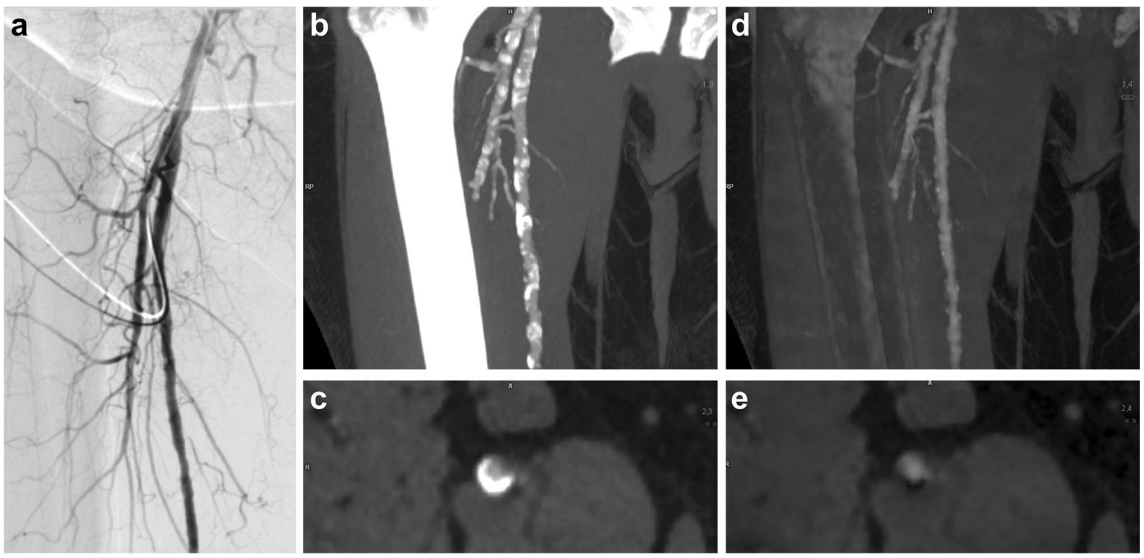

Fig. 4 Imaging studies of a 63-year-old woman with claudication and multiple calcified plaques in the right superficial femoral artery. Digital subtraction angiography showed no evidence of significant stenosis (**a**). The diffuse calcifications visible on standard dual-energy CT angiography maximum intensity projections (**b**) and multi-planar reformats (**c**) hamper the assessment of vessel lumina, as stenoses were overestimated and considered significant by both observers. Corresponding calcium-subtracted image series (**d**, **e**) enabled correct evaluation and rule-out of significant stenosis due to the complete subtraction of calcium and associated blooming artifacts (window width, 800 HU; level, 220 HU)

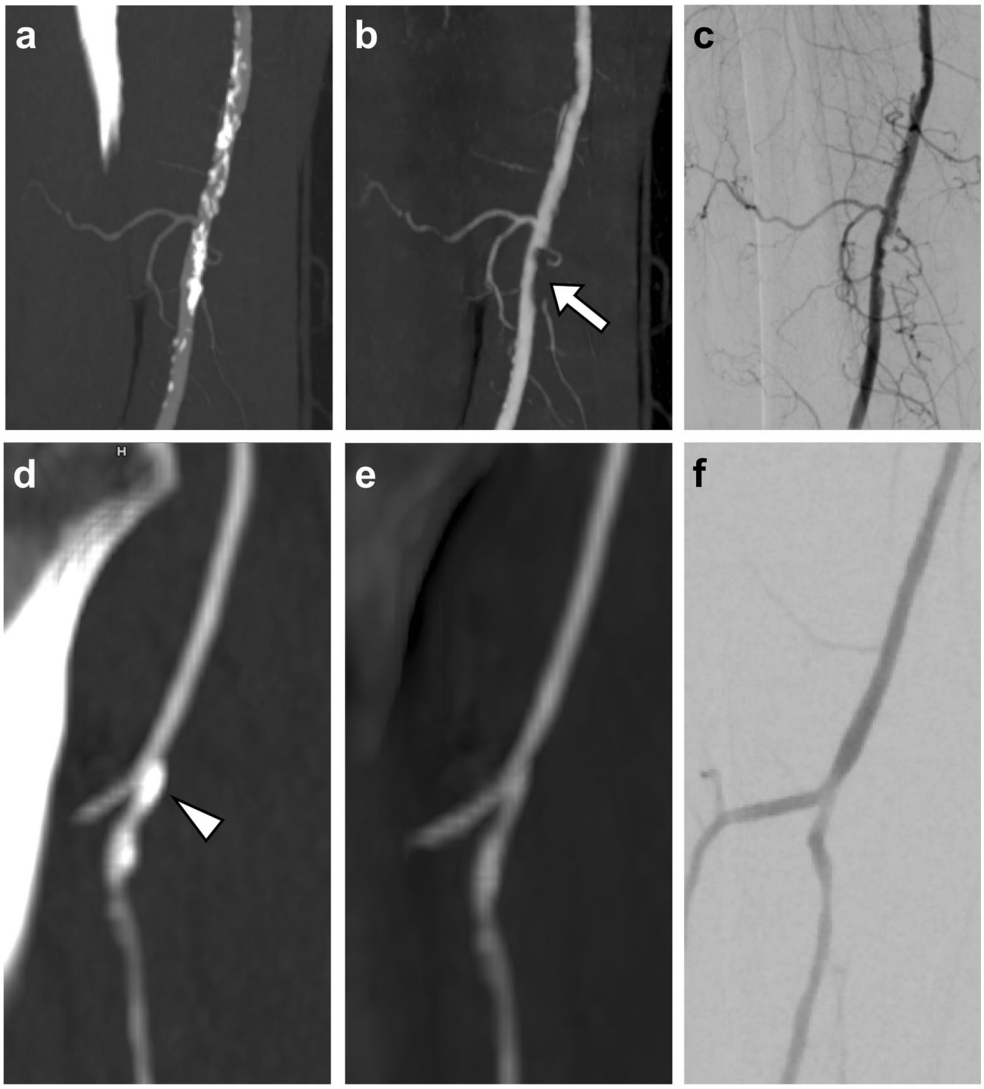

Fig. 5 Imaging studies of a 67-year-old woman with suspected peripheral artery disease. Standard dual-energy CT angiography maximum intensity projections showed severe calcifications in the right superficial femoral artery (**a**). The opacified arterial lumen is obscured and stenosis evaluation is impeded. The calcium-subtracted reconstructions (**b**) reveal one significant stenosis (*arrow*) confirmed by digital subtraction angiography (**c**). More distally, a focal stenosis in the right popliteal artery is visible on standard dual-energy CT angiography reconstructions (**d**), calcium-subtracted images (**e**), and digital subtraction angiography (**f**). The stenosis was erroneously rated significant (> 50%) on standard dual-energy CT angiography images (*arrowhead*), but correctly graded non-significant on calcium-subtracted reconstructions as confirmed by digital subtraction angiography (window width, 750 HU; level, 300 HU)

which influences luminal visualization [30], and the relatively long sampling window, accounting for motion artifacts [23]. In this context, additional diagnostic algorithms would be preferable in order to possibly determine, in advance, which patients can benefit from an invasive procedure and which patients can eventually avoid DSA.

Calcified atherosclerotic plaques frequently cause extensive blooming artifacts in CTA, which can obscure adjacent lumen and therefore lead to an overestimation of stenosis severity. Increasing the window level and width can help minimize the effect, however, at the cost of decreased iodine signal, which may hinder stenosis evaluation [3, 31]. The results of our study show that the CS algorithm resulted in higher diagnostic accuracy for the detection of arterial stenosis on DE-CTA of the lower extremity runoff using DSA as the reference standard, predominantly via greater specificity and PPV, when compared with the standard DE-CTA reconstructions. Furthermore, we found that the CS algorithm was superior in terms of objective image quality although there were significant differences in subjective image quality. Prior studies have shown multiple advantages of DE-CTA for improved vascular imaging [32], mainly by improving vascular attenuation [19, 33], as well as reducing blooming artifacts of calcified plaques [34] and stents [18]. Bone removal algorithms have also been evaluated as a potential approach for calcium subtraction, however, with varying evidence regarding the efficacy of this application. Poor results in small vessels have been reported, both in experimental models and in clinical studies [34–36]. One study investigated DE-CTA bone removal techniques in the lower extremities and found improved image quality and visualization of the residual lumen compared to standard image reconstructions. However, the impact on diagnostic accuracy for stenosis detection was not assessed [37]. Furthermore, residual inaccuracies have also been reported for bone removal algorithms in DE-CTA, especially for subtraction of calcified plaque in the lower extremities [34, 35]. It has been stated that these inaccuracies may be

caused by the failure of traditional material decomposition algorithms to recognize calcium as a primary material [15].

The feasibility of the CS algorithm in the setting of the coronary arteries has been demonstrated using third-generation DE-CTA data where improved luminal visualization and diagnostic observer confidence in the assessment of significant stenosis were found [16]. In another recent investigation, the CS algorithm was applied to the extracranial carotid arteries with DSA as the reference standard [15]. The authors reported fewer blooming artifacts and demonstrated the accurate removal of carotid calcified plaque using the CS algorithm, with no differences in quantitative stenosis measurements when compared with DSA. In accordance with these previous investigations, our study demonstrates that neither objective nor subjective measures of image quality are negatively affected by the modified CS technique when compared with standard image reconstruction. More importantly, our results extend this initial evidence, as they demonstrate a slight yet significant improvement in diagnostic accuracy for the detection of arterial stenosis in the lower extremities (96.5% vs. 93.1%). A potential explanation for this improved stenosis detection using CS image series may be a reduction of false positive findings in cases with calcified plaques, because overestimation of stenosis severity becomes more unlikely by selectively removing calcium and the associated blooming artifacts. However, one must consider that CTA has already reached high diagnostic performances in the assessment of PAD, with reported pooled sensitivity and specificity ≥ 95% [29, 38].

It is important to note that the CS algorithm did account for a slightly lower iodine attenuation compared to standard images (− 28%), in accordance with a previous investigation (− 18%) [16]. In addition, muscle attenuation was lowered to a greater extent, down to negative HU values (− 40 HU). These characteristics ultimately resulted in slight but significantly greater CNR when compared with standard reconstructions (15.3 vs. 13.5). The impact of the CS algorithm on attenuation density values should be taken into account especially in cases of relevant extravascular incidental findings, found in up to 15% of examinations [39]. In such scenarios, *standard* attenuation measurements are of paramount importance in the diagnostic process and the standard DE-CTA reconstruction should be preferred over the CS dataset. Therefore, despite the demonstrated added diagnostic value provided by the CS reconstruction images in the diagnosis of PAD, we believe that one should consider a combined approach incorporating both CS and standard reconstruction images in potential future clinical applications.

In addition to its retrospective design, the results of our study must be interpreted in the context of limitations. First, this preliminary investigation was designed as a single-center study. Another limitation of this study is that our results are currently applicable only to this vendor-specific CS algorithm and are based on a dedicated DE-CTA dataset. Lastly, qualitative scoring biases cannot be completely excluded, since it was inherently evident which image series were reconstructed with the CS algorithm despite randomization and independent observer evaluations.

In conclusion, we found that DE-CTA image series derived from a prototype modified three-material decomposition CS algorithm demonstrated improved diagnostic accuracy in the detection of significant stenosis on DE-CTA of the lower extremity runoff without impeding image quality when compared with standard reconstructions. The application of this algorithm in patients with heavily calcified vessels may be helpful in potentially reducing inconclusive CTA examinations and the need for subsequent invasive DSA.

Funding The authors state that this work has not received any funding.

Compliance with ethical standards

Guarantor The scientific guarantor of this publication is Prof. U. Joseph Schoepf.

Conflict of interest The authors of this manuscript declare relationships with the following companies: U.J.S. receives institutional research support from Astellas, Bayer, General Electric, and Siemens Healthineers. U.J.S. has received honoraria for speaking and consulting from Bayer, Guerbet, HeartFlow Inc., and Siemens Healthineers. C.N.D.C. receives institutional research support from Siemens Healthineers and speaking fees from Bayer. A.V.S. receives institutional research support from Siemens Healthineers. J.L.W. received speaking fees from Siemens Healthineers and General Electric. K.O., K.L.G., and B.S. are employees of Siemens Healthineers. M.H.A. received speaking fees from Siemens Healthineers and Bracco. All other authors declare that they have no conflict of interest.

Statistics and biometry One of the authors has significant statistical expertise.

Informed consent Written informed consent was waived by the Institutional Review Board.

Ethical approval Institutional Review Board approval was obtained.

Methodology
- retrospective
- diagnostic or prognostic study
- performed at one institution

References

1. Ouwendijk R, de Vries M, Pattynama PM et al (2005) Imaging peripheral arterial disease: a randomized controlled trial comparing contrast-enhanced MR angiography and multi-detector row CT angiography. Radiology 236:1094–1103
2. Ouwendijk R, Kock MC, Visser K, Pattynama PM, de Haan MW, Hunink MG (2005) Interobserver agreement for the interpretation of contrast-enhanced 3D MR angiography and MDCT angiography

in peripheral arterial disease. AJR Am J Roentgenol 185:1261–1267
3. Thomas C, Korn A, Ketelsen D et al (2010) Automatic lumen segmentation in calcified plaques: dual-energy CT versus standard reconstructions in comparison with digital subtraction angiography. AJR Am J Roentgenol 194:1590–1595
4. Sommer WH, Bamberg F, Johnson TR et al (2012) Diagnostic accuracy of dynamic computed tomographic angiographic of the lower leg in patients with critical limb ischemia. Invest Radiol 47: 325–331
5. Sandgaard NC, Diederichsen AC, Petersen H, Høilund-Carlsen PF, Mickley H (2012) Patients' views of cardiac computed tomography angiography compared with conventional coronary angiography. J Thorac Imaging 27:36–39
6. Iezzi R, Santoro M, Marano R et al (2012) Low-dose multidetector CT angiography in the evaluation of infrarenal aorta and peripheral arterial occlusive disease. Radiology 263:287–298
7. Kock MC, Adriaensen ME, Pattynama PM et al (2005) DSA versus multi-detector row CT angiography in peripheral arterial disease: randomized controlled trial. Radiology 237:727–737
8. Heijenbrok-Kal MH, Kock MC, Hunink MG (2007) Lower extremity arterial disease: multidetector CT angiography meta-analysis. Radiology 245:433–439
9. Schwarz F, Ruzsics B, Schoepf UJ et al (2008) Dual-energy CT of the heart–principles and protocols. Eur J Radiol 68:423–433
10. Vliegenthart R, Pelgrim GJ, Ebersberger U, Rowe GW, Oudkerk M, Schoepf UJ (2012) Dual-energy CT of the heart. AJR Am J Roentgenol 199:S54–S63
11. Albrecht MH, Trommer J, Wichmann JL et al (2016) Comprehensive comparison of virtual monoenergetic and linearly blended reconstruction techniques in third-generation dual-source dual-energy computed tomography angiography of the thorax and abdomen. Invest Radiol 51:582–590
12. Johnson TR, Krauss B, Sedlmair M et al (2007) Material differentiation by dual energy CT: initial experience. Eur Radiol 17:1510–1517
13. Schwarz F, Nance JW Jr, Ruzsics B, Bastarrika G, Sterzik A, Schoepf UJ (2012) Quantification of coronary artery calcium on the basis of dual-energy coronary CT angiography. Radiology 264:700–707
14. van Straten M, Schaap M, Dijkshoorn ML et al (2011) Automated bone removal in CT angiography: comparison of methods based on single energy and dual energy scans. Med Phys 38:6128–6137
15. Mannil M, Ramachandran J, Vittoria de Martini I et al (2017) Modified dual-energy algorithm for calcified plaque removal: evaluation in carotid computed tomography angiography and comparison with digital subtraction angiography. Invest Radiol 52:680–685
16. De Santis D, Jin KN, Schoepf UJ et al (2018) Heavily calcified coronary arteries: advanced calcium subtraction improves luminal visualization and diagnostic confidence in dual-energy coronary computed tomography angiography. Invest Radiol 53:103–109
17. Meyer M, Haubenreisser H, Schoepf UJ et al (2014) Closing in on the K edge: coronary CT angiography at 100, 80, and 70 kV-initial comparison of a second- versus a third-generation dual-source CT system. Radiology 273:373–382
18. Mangold S, De Cecco CN, Schoepf UJ et al (2016) A noise-optimized virtual monochromatic reconstruction algorithm improves stent visualization and diagnostic accuracy for detection of in-stent re-stenosis in lower extremity run-off CT angiography. Eur Radiol 26:4380–4389
19. Wichmann JL, Gillott MR, De Cecco CN et al (2016) Dual-energy computed tomography angiography of the lower extremity runoff: impact of noise-optimized virtual monochromatic imaging on image quality and diagnostic accuracy. Invest Radiol 51:139–146
20. Saltybaeva N, Jafari ME, Hupfer M, Kalender WA (2014) Estimates of effective dose for CT scans of the lower extremities. Radiology 273:153–159
21. Martin SS, Albrecht MH, Wichmann JL et al (2017) Value of a noise-optimized virtual monoenergetic reconstruction technique in dual-energy CT for planning of transcatheter aortic valve replacement. Eur Radiol 27:705–714
22. Genders TS, Spronk S, Stijnen T, Steyerberg EW, Lesaffre E, Hunink MG (2012) Methods for calculating sensitivity and specificity of clustered data: a tutorial. Radiology 265:910–916
23. Haneder S, Attenberger UI, Riffel P, Henzler T, Schoenberg SO, Michaely HJ (2011) Magnetic resonance angiography (MRA) of the calf station at 3.0 T: intraindividual comparison of non-enhanced ECG-gated flow-dependent MRA, continuous table movement MRA and time-resolved MRA. Eur Radiol 21:1452–1461
24. Pollak AW, Norton PT, Kramer CM (2012) Multimodality imaging of lower extremity peripheral arterial disease: current role and future directions. Circ Cardiovasc Imaging 5:797–807
25. Varga-Szemes A, Wichmann JL, Schoepf UJ et al (2017) Accuracy of noncontrast quiescent-interval single-shot lower extremity MR angiography versus CT angiography for diagnosis of peripheral artery disease: comparison with digital subtraction angiography. JACC Cardiovasc Imaging 10:1116–1124
26. Ascher E, Mazzariol F, Hingorani A, Salles-Cunha S, Gade P (1999) The use of duplex ultrasound arterial mapping as an alternative to conventional arteriography for primary and secondary infrapopliteal bypasses. Am J Surg 178:162–165
27. Aboyans V, Ricco JB, Bartelink MEL et al (2018) 2017 ESC guidelines on the diagnosis and treatment of peripheral arterial diseases, in collaboration with the European Society for Vascular Surgery (ESVS): document covering atherosclerotic disease of extracranial carotid and vertebral, mesenteric, renal, upper and lower extremity arteries endorsed by: the European Stroke Organization (ESO) The Task Force for the Diagnosis and Treatment of Peripheral Arterial Diseases of the European Society of Cardiology (ESC) and of the European Society for Vascular Surgery (ESVS). Eur Heart J 39: 763–816
28. Gerhard-Herman MD, Gornik HL, Barrett C et al (2017) 2016 AHA/ACC guideline on the management of patients with lower extremity peripheral artery disease: executive summary: a report of the American College of Cardiology/American Heart Association Task Force on Clinical Practice Guidelines. Circulation 135:e686–e725
29. Jens S, Koelemay MJ, Reekers JA, Bipat S (2013) Diagnostic performance of computed tomography angiography and contrast-enhanced magnetic resonance angiography in patients with critical limb ischaemia and intermittent claudication: systematic review and meta-analysis. Eur Radiol 23:3104–3114
30. Lim RP, Hecht EM, Xu J et al (2008) 3D nongadolinium-enhanced ECG-gated MRA of the distal lower extremities: preliminary clinical experience. J Magn Reson Imaging 28:181–189
31. Klink T, Wilhelm T, Roth C, Heverhagen JT (2017) Dual-energy CTA in patients with symptomatic peripheral arterial occlusive disease: study of diagnostic accuracy and impeding factors. Rofo 189: 441–452
32. De Santis D, Eid M, De Cecco CN et al (2018) Dual-energy computed tomography in cardiothoracic vascular imaging. Radiol Clin North Am 56:521–534
33. Albrecht MH, Scholtz JE, Hüsers K et al (2016) Advanced image-based virtual monoenergetic dual-energy CT angiography of the abdomen: optimization of kiloelectron volt settings to improve image contrast. Eur Radiol 26:1863–1870
34. Meyer BC, Werncke T, Hopfenmuller W, Raatschen HJ, Wolf KJ, Albrecht T (2008) Dual energy CT of peripheral arteries: effect of

automatic bone and plaque removal on image quality and grading of stenoses. Eur J Radiol 68:414–422
35. Tran DN, Straka M, Roos JE, Napel S, Fleischmann D (2009) Dual-energy CT discrimination of iodine and calcium: experimental results and implications for lower extremity CT angiography. Acad Radiol 16:160–171
36. Werncke T, Albrecht T, Wolf KJ, Meyer BC (2010) Dual energy CT of the peripheral arteries: a phantom study to assess the effect of automatic plaque removal on stenosis grading. Rofo 182:682–689
37. Sommer WH, Johnson TR, Becker CR et al (2009) The value of dual-energy bone removal in maximum intensity projections of lower extremity computed tomography angiography. Invest Radiol 44:285–292
38. Met R, Bipat S, Legemate DA, Reekers JA, Koelemay MJ (2009) Diagnostic performance of computed tomography angiography in peripheral arterial disease: a systematic review and meta-analysis. JAMA 301:415–424
39. Naidu SG, Hara AK, Brandis AR, Stone WM (2010) Incidence of highly important extravascular findings detected on CT angiography of the abdominal aorta and the lower extremities. AJR Am J Roentgenol 194:1630–1634